

DcERF109 regulates shoot branching by participating in strigolactone signal transduction in *Dendrobium catenatum*

Yuliang Han^{1†} | Juncheng Zhang^{1†} | Siqi Zhang¹ | Lijun Xiang² |
Zhonghua Lei² | Qixiu Huang² | Huizhong Wang¹ | Tao Chen¹ | Maohong Cai¹ 

¹Zhejiang Provincial Key Laboratory for Genetic Improvement and Quality Control of Medicinal Plants, College of Life and Environmental Science, Hangzhou Normal University, Hangzhou, China

²Institute of Economic Crops, Xinjiang Academy of Agricultural Sciences, China

Correspondence

Maohong Cai,
Email: caimaohong@hznu.edu.cn

Funding information

Scientific Research Foundation for Scholars of HZNU, Grant/Award Number: 2019QDL015

Edited by J. Chen

Abstract

Shoot branching fundamentally influences plant architecture and agricultural yield. However, research on shoot branching in *Dendrobium catenatum*, an endangered medicinal plant in China, remains limited. In this study, we identified a transcription factor *DcERF109* as a key player in shoot branching by regulating the expression of strigolactone (SL) receptors *DWARF 14 (D14)/ DECREASED APICAL DOMINANCE 2 (DAD2)*. The treatment of *D. catenatum* seedlings with GR24^{rac}/TIS108 revealed that SL can significantly repress the shoot branching in *D. catenatum*. The expression of *DcERF109* in multi-branched seedlings is significantly higher than that of single-branched seedlings. Ectopic expression in *Arabidopsis thaliana* demonstrated that overexpression of *DcERF109* resulted in significant shoot branches increasing and dwarfing. Molecular and biochemical assays demonstrated that *DcERF109* can directly bind to the promoters of *AtD14* and *DcDAD2.2* to inhibit their expression, thereby positively regulating shoot branching. Inhibition of *DcERF109* by virus-induced gene silencing (VIGS) resulted in decreased shoot branching and improved *DcDAD2.2* expression. Moreover, overexpression of *DpERF109* in *A. thaliana*, the homologous gene of *DcERF109* in *Dendrobium primulinum*, showed similar phenotypes to *DcERF109* in shoot branch and plant height. Collectively, these findings shed new insights into the regulation of plant shoot branching and provide a theoretical basis for improving the yield of *D. catenatum*.

1 | INTRODUCTION

Shoot branching is an important agronomic trait that affects plant architecture and yield potential, which is mainly controlled by a complex interplay of hormonal signalling, developmental processes, and environmental cues. Strigolactones (SLs) have emerged as a novel class of phytohormones with a multifaceted role in the modulation of shoot branching. Additionally, SLs serve as vital rhizosphere signals, orchestrating the interactions between plants and fungal partners, as well as with parasitic weeds. (Cheng et al., 2017; Q. Wang et al., 2022; Xu et al., 2021). Recent advancements have elucidated

considerable portions of the SL biosynthetic pathway in plants. Firstly, all-trans-carotene was isomerized into 9-cis-carotene by beta-carotene isomerase *DWARF 27 (D27)*. Sequential action of carotenoid cleavage dioxygenases *CCD7* and *CCD8* results in the formation of the key precursor carlactone (CL) through bond cleavage and oxidative rearrangement. CL is subsequently translocated to the cytoplasm and further oxidized and modified by cytochrome P450 enzymes (e.g., *MAX1*, *CYP722C*) anchored to the endoplasmic reticulum, thus generating bioactive strigolactones (Mashiguchi et al., 2021). In plants, *D14/DAD2* functions as an α/β hydrolase, which serves as a non-canonical hormone receptor with the dual function of producing and perceiving the active SL (Yao et al., 2016). *D14/DAD2*, transported through the phloem to the axillary bud, plays a pivotal role in

[†] These authors contributed equally to this work.

facilitating the full function of strigolactones in inhibiting shoot branching (Kameoka et al., 2016). Upon binding to SLs, the receptor protein D14/DAD2 triggers the assembly of a complex of SCF^{D3/MAX2}-D14/DAD2 to degrade the repressor protein DWARF 53 (D53) and its homologs SUPPRESSOR OF MAX2-LIKE 6, 7 and 8 (SMXL6, SMXL7 and SMXL8) via the 26S proteasome pathway, and ultimately to relieve inhibition of downstream genes (Jiang et al., 2013; Wang et al., 2015; L. Wang et al., 2020).

The AP2/ERF superfamily encompasses a diverse group of transcription factors that act as key factors in plant developmental regulation and the response to biotic and abiotic stresses (Licausi et al., 2013). Prior studies indicate a strong association between the AP2/ERF family and plant branching. For instance, overexpression of MtRAVs in *A. thaliana* increased the number of branches and stress tolerance (S. Wang et al., 2020). It has been reported that *AtERF12* negatively regulated plant branching, and its homologous gene *DUO-B1* in wheat has also been shown to affect the spike number (Chandler and Werr, 2020; Y. Wang et al., 2022). In addition, Several AP2/ERF-like genes are found to be significantly enriched during the domestication process of rice, suggesting a close linkage to the regulation of rice branching patterns by analyzing the transcriptome differences between domesticated rice and wild type (Harrop et al., 2019).

Dendrobium catenatum, a member of the Orchidaceae family, is a genus of herbaceous plants recognized for its stems that are rich in a variety of bioactive compounds, such as polysaccharides and flavonoids, which are beneficial to health (Wang et al., 2021; Yan et al., 2015). Given its pharmacological significance, *D. catenatum* is esteemed as an important medicinal plant in China and possesses substantial commercial value globally. The stem of *D. catenatum* serves as the synthesis and storage site of secondary metabolites, and its quantity has a great influence on the overall value of the plant. However, the mechanistic understanding of shoot branching regulation in *D. catenatum* remains relatively underexplored.

Here, we identified a novel member of the AP2/ERF family transcription factor *DcERF109*, which was highly expressed in the stem base of multi-shoot branched seedlings compared to single-shoot branched seedlings. The expression profile of *DcERF109* in different tissues showed that *DcERF109* is expressed ubiquitously in all tissues, with the highest expression in the stem base. Transient expression in protoplasts of *D. catenatum* and tobacco leaves showed that *DcERF109* localized in the nucleus. To verify the function of *DcERF109* in the regulation of shoot branching, we generated *DcERF109* overexpression transgenic plants in *A. thaliana*. The transgenic lines displayed enhanced shoot branching coupled with pronounced dwarfism, a clear demonstration of the phenotypic influence of *DcERF109*. Further studies confirmed that *DcERF109* represses the expression of *AtD14* and *DcDAD2.2* by directly binding to their promoter, thereby controlling shoot branching via involvement in the strigolactone pathway. Silencing of *DcERF109* in *D. catenatum* seedlings by the VIGS system significantly decreased the emergence of new shoot branches. Altogether, our investigations have enriched the current understanding of the ERF gene family function and

the regulatory mechanism of plant branching. It may potentially contribute to the enhancement of the quality and economic value of *D. catenatum*.

2 | MATERIALS AND METHODS

2.1 | Plant materials and growth conditions

'Honggan ruanjiao', a well-known *D. catenatum* variety, was used in this study. Three-month-old tissue culture seedlings were cultured in a growth medium (3.21 g L⁻¹ B5 medium powder, 0.5 mg L⁻¹ NAA, 10% banana extract, 30 g L⁻¹ sucrose) and grew at 25°C. The photoperiod is 12/12 h light/dark.

For *A. thaliana* transgenic plants, the *Agrobacterium tumefaciens*-mediated flower dip method was used to obtain transgenic *A. thaliana* lines. Detailed procedures were performed following previously validated mature transgenic protocols (Bechtold and Pelletier, 1998; Zhang et al., 2006). The Columbia (Col-0) was used as a wild type. For the cultivation of *A. thaliana*, sterilized seeds were soaked in ddH₂O and incubated at 4°C for 3 days. They were then placed on Petri dishes containing 1/2 MS, 1% sucrose, and 1.2% agar, and grew in a culture chamber with 60–80 μmol m⁻² s⁻¹ at 16/8 h light/dark and 22°C (Yu et al., 2012).

2.2 | RNA extraction and quantitative real-time PCR (RT-qPCR)

Total RNA was extracted from *D. catenatum* seedlings by using the Total RNA Extract Reagent (Coolaber). cDNAs were synthesized by HiScript II Q Select RT SuperMix for RT-qPCR (Vazyme). RT-qPCR was performed on a CFX384 real-time system (BIO-RAD) with ChamQ Universal SYBR qPCR Master Mix (Vazyme). Primers used in this assay are listed in Table S1.

2.3 | Subcellular localization of DcERF109

The full-length coding sequences of *DcERF109* were amplified and cloned into the pEarleyGate 101 vector to produce the *DcERF109*-GFP fusion protein. To observe the localization in protoplasts of *D. catenatum*, the matured leaves of six-month-old seedlings were used for protoplast transformation. The detailed method was referred to in a previous study (Chai et al., 2007; Han et al., 2022). Briefly, 10 μg plasmid was transformed into 100 μL protoplast suspension, and the fluorescence signal was detected by a confocal microscope after 12 h incubation.

For transient expression, the activated *EHA105* agrobacterium containing the constructed plasmids was incubated with infection solution (10 mM MES, 10 mM MgCl₂, and 200 μM AS) for at least 30 min and then injected into the four-week-old young leaves of *N. benthamiana* (tobacco). After about 48–72 h incubation, the

fluorescence was detected at 488 and 560 nm using a confocal microscope.

2.4 | Yeast one-hybrid and Yeast Two-Hybrid (Y2H) Assays

For Y1H, the full-length coding region of *DcERF109* was cloned into the pB42AD vector. The full promoter (~2 kb) of *AtD14/DcDAD2.2* and their truncated fragments, including P1-P4, were cloned into the pLacZi vector, respectively (Lin et al., 2007). The above constructs were co-transformed into EGY48 and selected on SD/-Ura/-Trp agar medium (Coolaber). Colonies were finally plated onto SD/-Ura/-Trp agar medium containing raffinose, galactose, and X-Gal (5-bromo-4-chloro-3-indolyl-b-D-galactopyranoside) for binding strength detection. Primers used in this assay are listed in Table S1.

For Y2H, the full-length CDS and three truncated fragments of *DcERF109* were cloned into the pGBKT7 vector. The above constructs were co-transformed into AH109 with empty pGADT7 using the Yeastmaker Yeast Transformation System (Clontech). Transformation cells were plated on SD/-Trp/-Leu medium (DDO) to screen positive clones. After 3 days, positive clones were transferred to SD/-Ade/-His/-Leu/-Trp dropout medium (QDO) to detect self-activation. Primers used in this assay are listed in Table S1.

2.5 | Luciferase reporter assays

For luciferase reporter assay (Xie et al., 2017), the full-length coding region of *DcERF109* was cloned into pGWB512 to generate the *p35S:DcERF109-Flag* effector construct. The promoter of *AtD14* and *DcDAD2.2* upstream 2000 bp of the ATG starting codon and their truncated fragments (P1-P4) were ligated into the pGreenII0800-LUC vector to generate the corresponding reporter constructs. These constructed plasmids were introduced into *Agrobacterium* strain EHA105. The specific methods refer to the above tobacco leaves transient expression. After 3 days, the injected leaves were sprayed with 1 mmol/L luciferin (E1601, Promega) for 1 min, and luciferase activities were measured using the Plant Living Imaging System (Berthold). Primers used for this assay are listed in Table S1.

2.6 | GUS staining

For GUS activity detection, the promoter of *DcERF109* was ligated into the pCambia1381Z vector to generate the corresponding reporter construct. This construct was introduced into *A. thaliana* wild-type plants (Col-0) by *Agrobacterium*-mediated infiltration (Bechtold and Pelletier, 1998). Transgenic plants were selected on MS agar plates containing 50 $\mu\text{g mL}^{-1}$ hygromycin and stained in GUS staining buffer for 12 h at 37°C. Stained seedlings were first decolorized with 75% ethanol and then observed and recorded with a camera. GUS staining was done with the Coolaber reagent, as stated in the manual.

2.7 | Virus-induced gene silencing (VIGS) of *DcERF109* in *D. catenatum*

DcERF109 was silenced using the VIGS system mediated by tobacco rattle virus (TRV) in this study. A 305 bp fragment of *DcERF109* was amplified and inserted into the pTRV2 to form the pTRV2-*DcERF109* construct. pTRV2, pTRV2-*DcERF109* and pTRV1 were transformed individually into *Agrobacterium* EHA105. The *Agrobacterium* strains were shaken in LB liquid medium overnight, collected by centrifugation, and resuspended to an OD₆₀₀ of 1.0 in infiltration buffer (10 mM MES, 10 mM MgCl₂, and 0.2 mM acetosyringone). Finally, two *Agrobacterium* suspensions containing (1) pTRV1 and pTRV2-*DcERF109* and (2) pTRV1 and pTRV2 in a 1:1 (v/v) ratio were prepared.

D. catenatum seedlings were infected when they were about 10 cm in length, and they should be made sure they have not sprouted new stem branches. Several wounds were carefully scratched on their stems with a blade to facilitate infection. They were then soaked in infiltration buffer for 3 h in the dark and applied vacuum to -0.08 MPa for 3 min, abruptly breaking the vacuum every 1 min by quickly unplugging the vacuum source from the desiccator. After soaking for an additional 6–8 h in the dark, the seedlings were transferred to the nutrient soil containing pine bark for 15 days.

2.8 | Sequence alignment and domain analysis

All available *ERF109* homologous gene sequences were downloaded from NCBI (<https://www.ncbi.nlm.nih.gov/>). The Batch Web CD-Search tool (<https://www.ncbi.nlm.nih.gov/Structure/bwrpsb/bwrpsb.cgi>) (Lu et al., 2020) was used to perform domain analysis of all downloaded proteins and visualized by TBtools software (v1.113) (Chen et al., 2020). Sequence alignment and phylogenetic tree completed by the MEGA X software (Kumar et al., 2018).

3 | RESULTS

3.1 | SL analogues GR24^{rac} and its inhibitors TIS108 significantly affect the shoot branches of *D. catenatum*

SL signals are known to regulate the number of shoot branches in various plant species (de Jong et al., 2014; Kerr et al., 2021; Liang et al., 2010). To test if SL has functions in controlling shoot branching of *D. catenatum*, we employed the synthetic SL analogue GR24^{rac} and the SL biosynthesis inhibitor TIS108. The two compounds were added to the growth media for *D. catenatum* seedling treatment. As shown in Figure 1A, compared to the control group, the emergence of new shoot branches of seedlings treated with GR24^{rac} was significantly reduced, whereas TIS108-treated seedlings manifested an increase in shoot branches. This distinction became more pronounced after an extended culture period of 70 days (Figure 1B). These results suggested that SL plays a vital function in inhibiting the shoot branching

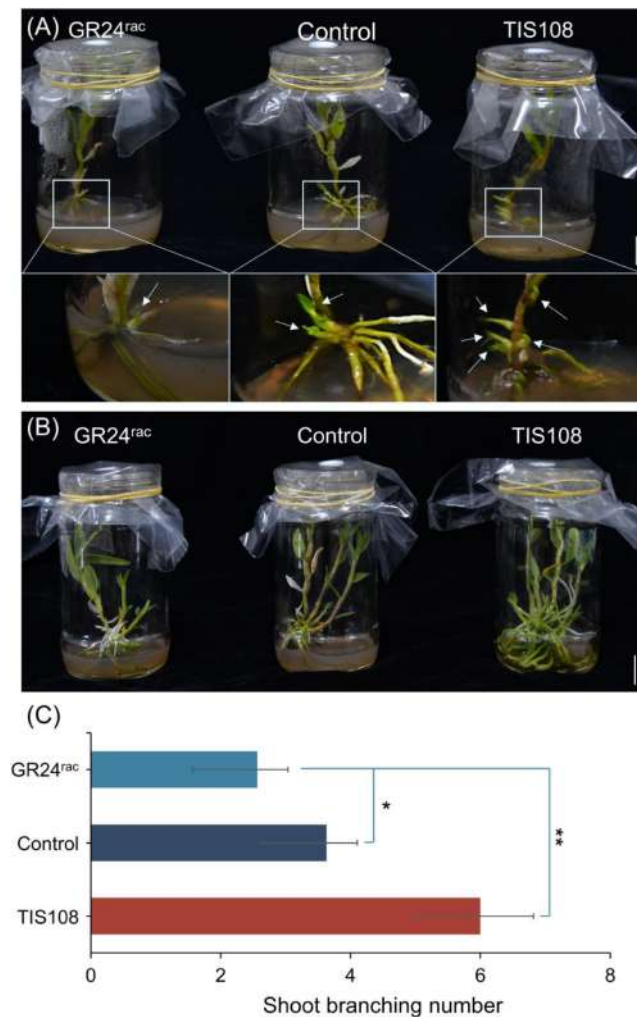


FIGURE 1 GR24^{rac} and TIS108 affect *D. catenatum* shoot branches.

A, Top row: Treatment of *D. catenatum* seedlings by 5 μ M GR24^{rac} and 3 μ M TIS108 ($n = 3$) for 30 days. Bottom row: Enlarged images of the white box in the top row. Bar = 2 cm. **B**, GR24^{rac}/TIS108 treatment of *D. catenatum* seedlings for 70 days. Bar = 2 cm. **C**, Statistics of the number of shoot branches in different treatment groups. Values are presented as means \pm SD (* $p < 0.05$, ** $p < 0.01$, Student's *t*-test).

in *D. catenatum*, which revealed the conservative function of SL in regulating plant shoot branching.

3.2 | Shoot branching of *D. catenatum* is closely related to SL signal and *DcERF109* expression

D14/DAD2 serves as the core sensing receptor in the SL signalling cascade. To further investigate the correlation between the shoot branching and SL signals in *D. catenatum*, two types of seedlings (single-shoot branched and multi-shoot branched) were selected (Figure 2A). RNA was extracted from the base of their stems for the expression evaluation of two *D14* homologous genes *DAD2.1*

(LOC110104816) and *DAD2.2* (LOC110095742) in *D. catenatum* (Simons et al., 2007; Hamiaux et al., 2012). RT-qPCR analysis indicated that the expression level of *DcDAD2.2* in the multi-shoot branched plants significantly decreased compared to single-shoot branched plants, whereas no significant change was observed for *DcDAD2.1*. (Figure 2B).

Based on the AP2/ERF gene family transcriptome data that we compiled previously (Han et al., 2022), 10 AP2/ERF family genes were selected to assess their expression patterns in these two samples. The results showed that the expression levels of *DcERF109*, *DcERF5*, and *DcERF71* were higher in the stem base of multi-shoot branched plants, and the expression levels of *DcERF105*, *DcERF25*, and *DcPT15* were higher in single shoot branched plants (Figure 2C). Notably, *DcERF109* stood out with an approximately 10-fold upsurge in expression within in multi-shoot branched plants. Tissue expression analysis revealed that *DcERF109* was expressed ubiquitously in all tissues, with predominant expression at the stem base of *D. catenatum* (Figure 2D). Furthermore, the *pDcERF109::GUS* transgenic plants also showed that *DcERF109* has strong expression in rosette base and roots (Figure S1). These data indicated that *DcERF109* may play a vital role in controlling the shoot branching of *D. catenatum*.

3.3 | *DcERF109* encodes a nuclear-localized transcription factor

Our previous investigations showed that *DcERF109* encodes an AP2/ERF transcription factor with a conserved AP2 domain (Han et al., 2022) (Figure 3A). To elucidate the function of *DcERF109*, we generated *DcERF109*-GFP fusion construct and transferred it into protoplasts of *D. catenatum* and *N. benthamiana* (tobacco) leaves through transient transformation assay. Free GFP was used as control. Consistent with the characteristics of transcription factors, the *DcERF109*-GFP fusion protein only appeared exclusively in the nucleus (Figure 3B). Transactivation activity assay showed that *DcERF109* had self-activating properties (Figure 3C), and the self-activating properties existed in the N terminal (1–115 aa) and C terminal (180–232 aa) segments, while not the middle region (116–179 aa), which encompasses the AP2 domain.

3.4 | Overexpression of *DcERF109* in *A. thaliana* results in dwarfing and multi-shoot branched phenotype

Due to the inherent challenges associated with generating stably transformed *D. catenatum*, we ectopically expressed *DcERF109* in *A. thaliana* ecotype Col-0 to reveal the effect of *DcERF109* on plant shoot branching. The expression levels of *DcERF109* in positive transgenic plants were detected by RT-qPCR (Figure S2), and three transgenic lines with moderate expression levels (OE1, OE2 and OE3) were selected for further analysis (Figure 4A). Phenotype assessments revealed that the shoot branching number of transgenic lines has

FIGURE 2 Expression analysis of *DAD2.1*, *DAD2.2*, and 10 AP2/ERF family genes in single and multi-branching plants.

A, Plant phenotypes of single-shoot branched and multi-shoot branched *D. catenatum* seedlings. Bar = 1 cm. **B**, the Expression level of two *D14* homologous genes in *D. catenatum* at the stem base of single-shoot branched and multi-shoot branched plants. Values are presented as means \pm SD (* $p < 0.05$, ** $p < 0.01$, Student's *t*-test). **C**, Expression patterns of selected AP2/ERF family genes between single-shoot branched and multi-shoot branched plants. Values are presented as means \pm SD (* $p < 0.05$, ** $p < 0.01$, Student's *t*-test). **D**, Cartoon heat map of *DcERF109* in different parts of *D. catenatum*. *DcACTIN2* was used as an internal control. Values are presented as means \pm SD (n = 3, * $p < 0.05$, ** $p < 0.01$, Student's *t*-test).

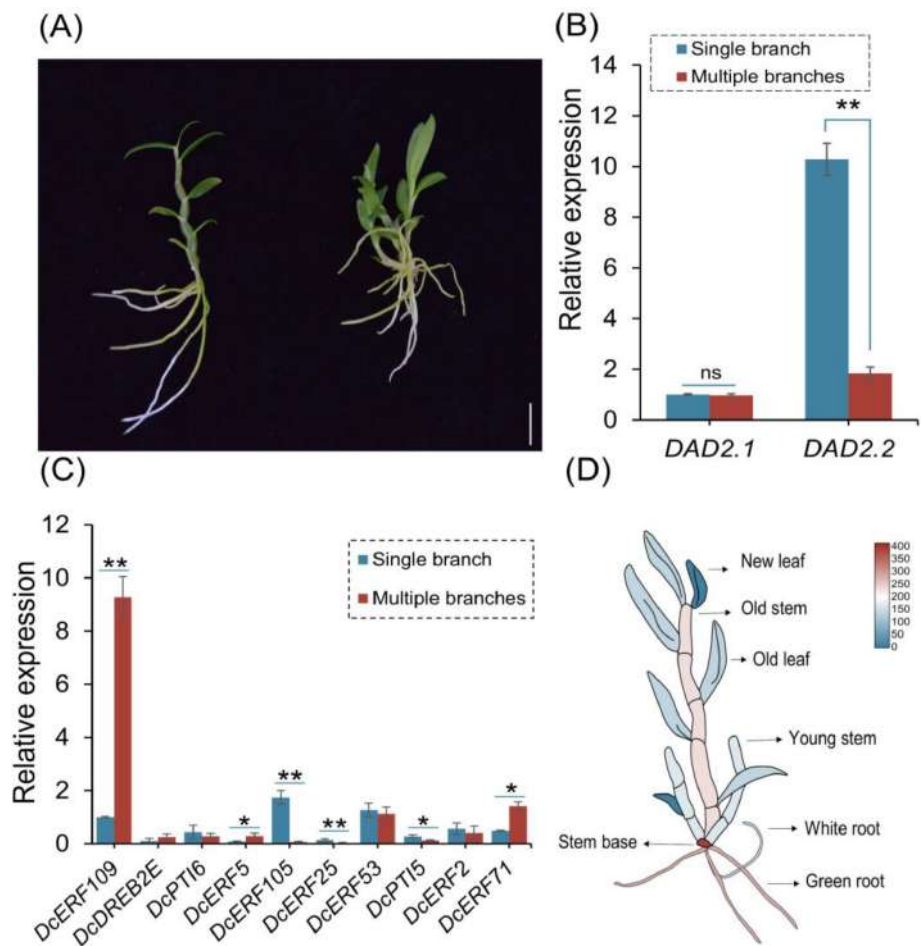
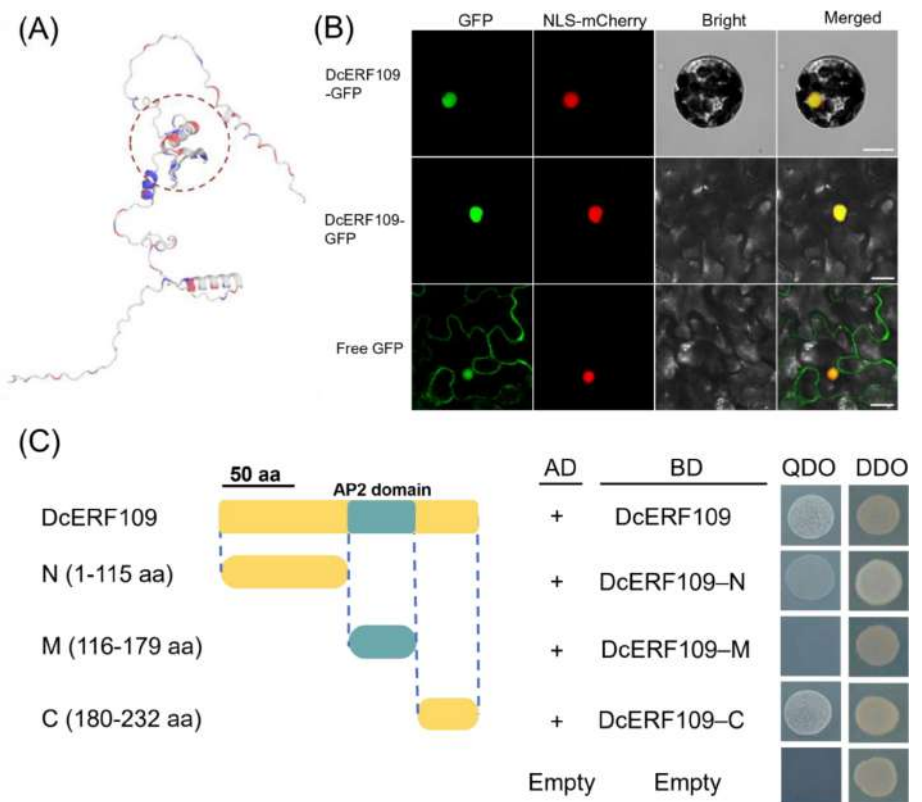


FIGURE 3 *DcERF109* exhibits significant transcription factor characteristics.

A, Structure model of *DcERF109*. The red circle indicates the AP2 domain position. **B**, Subcellular localization of *DcERF109*-GFP protein in *D. catenatum* protoplasts (first row) and the leaf cells of tobacco (second row). Free GFP was used as control (third row). NLS-mCherry was used as a nuclear marker. Bars = 20 μ m. The fluorescence signals were detected by confocal microscope. **C**, Yeast two-hybrid validation of *DcERF109* self-activation regions. The transformed yeast cells were plated on DDO (SD/-Trp/-Leu) and QDO (SD/-Trp/-Leu/-His/-Ade). Empty pGADT7 and pGBKT7 were co-transformed as negative control.



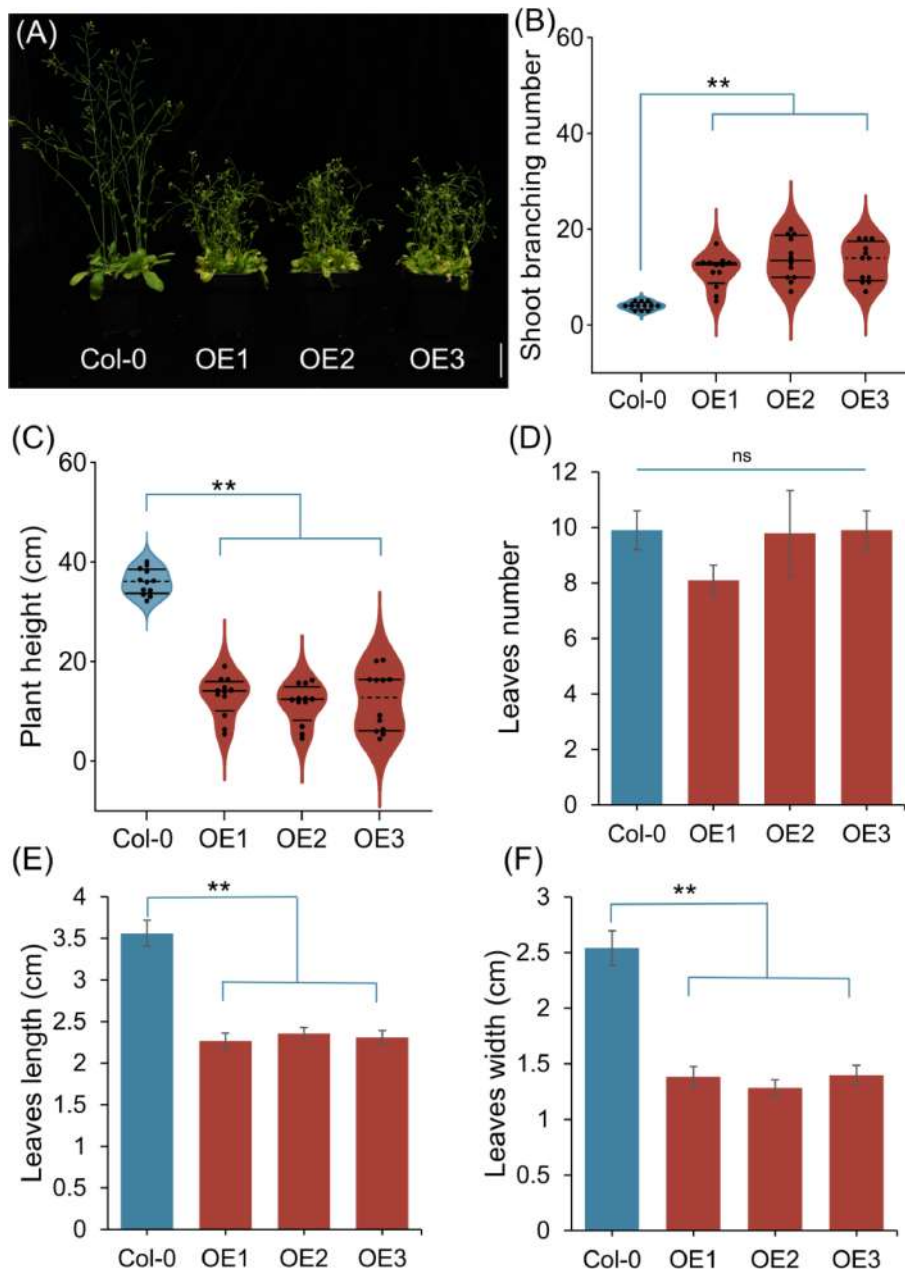


FIGURE 4 Plant phenotypes of *DcERF109* overexpression lines in *Arabidopsis*.

A, Excessive shoot branches phenotype of 3 representative *DcERF109* transgenic lines at a mature stage. Scale bar = 5 cm. **B-F**, Statistics results of the shoot branching number (**B**), plant height (**C**), leaves number (**D**), leaves length (**E**), and leaves width (**F**) of Col-0 and transgenic plants. Values are presented as means \pm SD ($n = 12$ * $p < 0.05$, ** $p < 0.01$, Student's *t*-test).

significantly increased and meanwhile the plant height was reduced (Figure 4A-C). These data were consistent with the high expression of *DcERF109* in multi-branched seedlings (Figure 2C), which confirms that *DcERF109* regulates the number of shoot branches. Leaf statistics showed that overexpression of *DcERF109* in *A. thaliana* has almost no difference in leaf number compared to the wild-type (Figure 4D). However, there are significant changes in leaf size, including leaf width and leaf length since the lotus period (Figure 4E,F and S3A,B). In addition, we also noticed that the root length and siliques of the *DcERF109*-OE lines were shorter than Col-0 (Figure S3C-D).

By checking the expression levels of *DcERF109* in transgenic lines, we found that some lines had extremely high expression levels (Figure S2). Three representative lines, OE4, OE5, and OE6, were selected for further analysis. As shown in Figure S4A, they appeared

to be a more severe dwarf and bushy phenotype. Statistical results demonstrated that the height of these lines was only 6 cm, while the height of OE1-OE3 and wild type was more than 20 cm and 30 cm, respectively (Figure 4C and Figure S4B). The shoot branch number was also much more than the wild type (Figure S4C). All these results indicated that *DcERF109* affected plant shoot branching and height in a dose-dependent manner.

3.5 | *DcERF109* binds to the *AtD14/DcDAD2.2* promoters to inhibit their expression

Strigolactone esterase D14/DAD2 is an α/β -hydrolase that can sense and cleave SLs. The RT-qPCR results have shown that *DcERF109* was

up-regulated in the stem base of multi-shoot branched seedlings compared to single-branched seedlings, while the expression level of *DcDAD2.2* was extremely down-regulated at the same part (Figure 2B,C). The expression of *AtD14* also significantly decreased in the *DcERF109*-OE transgenic lines (Figure S5). Based on the above results, we speculate that *DcERF109* may directly regulate the expression of *AtD14* and *DcDAD2.2*. Yeast-one-hybrid (Y1H) assay was performed, and results showed that *DcERF109* can bind directly to the promoter of *AtD14* and *DcDAD2.2* (Figure 5A). To further confirm the binding region, we divided the two promoters into four fragments and named them P1-P4 respectively (Figure 5B). The Y1H results showed that *DcERF109* protein bound strongly with P4 segments of both *AtD14* and *DcDAD2.2* promoters (Figure 5C).

To further reveal the regulation mechanism of *DcERF109* on *AtD14/DcDAD2.2*, luciferase reporter assays were performed. We transformed sets of construct combinations into young tobacco leaves to test the transcriptional effect of *DcERF109* protein on *AtD14/DcDAD2.2* expression. The activity of luciferase driven by *AtD14* and

promoter was significantly decreased when the *DcERF109*-Flag protein was added (Figure 5D), indicating that *DcERF109* had transcription repression activity on *AtD14* expression. Similar results were observed within *DcDAD2.2* expression (Figure 5E). To further investigate the same effect on P4 fragments, we replaced the full-length promoter with the P4 fragment in luciferase reporter assays. As shown in Figure 5F and G, the expression levels of luciferase were repressed more significantly. The Y1H and luciferase reporter assay results suggested that *DcERF109* represses the expression of *AtD14* and *DcDAD2.2* by directly binding to their promoters.

3.6 | *DcERF109* silenced seedlings had fewer shoot branches

Based on the fact that *DcERF109* overexpression in *A. thaliana* developed more shoot branches, we hypothesized that *DcERF109* has a similar function in *D. catenatum*. To verify our hypothesis, *DcERF109*

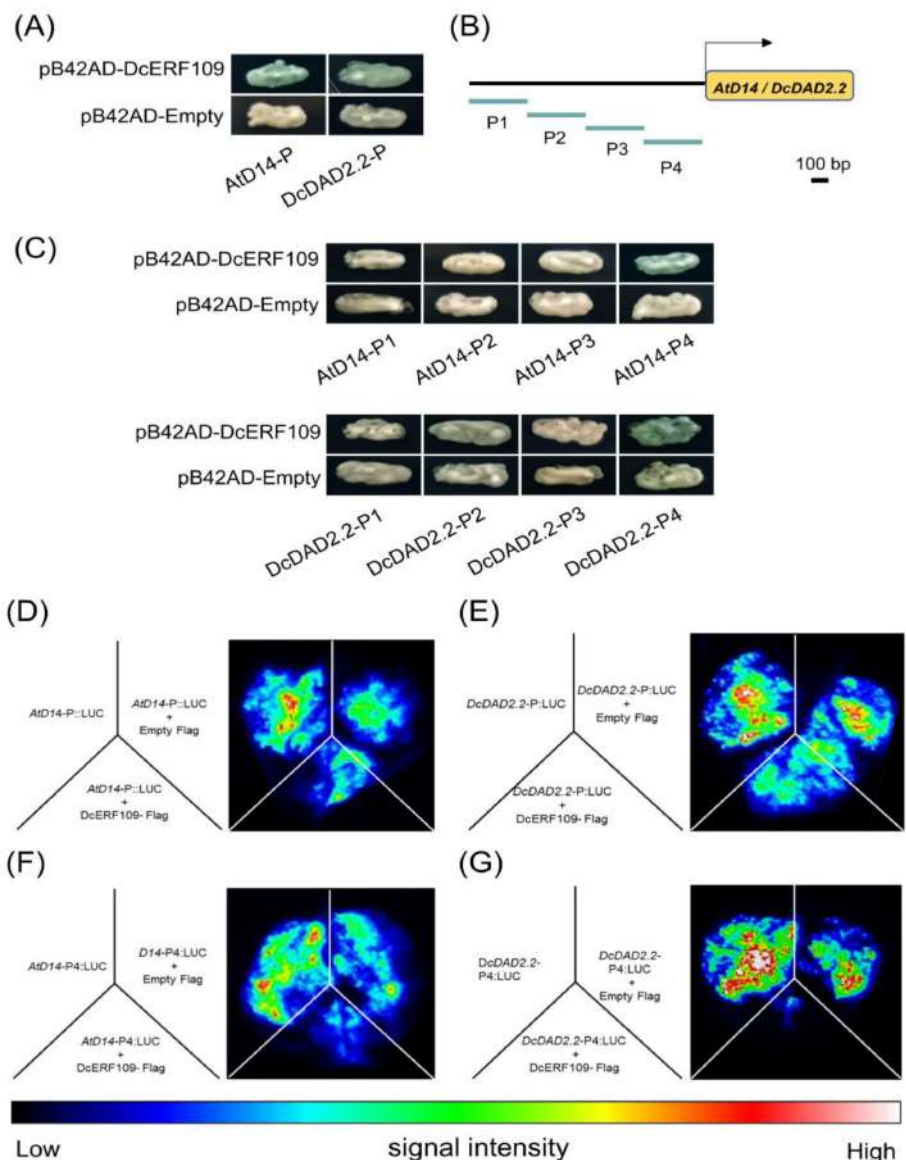


FIGURE 5 *DcERF109* directly bound to promoters of *AtD14* and *DcDAD2.2* and repressed their expression. **A**, Y1H showed that *DcERF109* can bind directly to the promoter of *AtD14* and *DcDAD2.2*. **B**, Schematic diagram of *AtD14/DcDAD2.2* promoter. 2000 bp upstream of the ATG start code of each gene were used as promoters. Each of the P1-P4 fragment lengths is about 500 bp. **C**, Y1H results indicated that *DcERF109* preferentially bound to the P4 segment of the *AtD14/DcDAD2.2* promoter. **D**, the expression repression effects of *DcERF109* on the full-length promoter of *AtD14*. **E**, the expression repression effects of *DcERF109* on the full-length promoter of *DcDAD2.2*. **F**, the expression repression effects of *DcERF109* on *AtD14*-P4. **G**, the expression repression effects of *DcERF109* on *DcDAD2.2*-P4.

was silenced using VIGS in 23 *D. catenatum* seedlings, and another 23 seedlings were used as control. Representative *DcERF109* silenced seedlings were shown in Figure 6A. After 15 days of infection, 10 (43.48%) of the control seedlings began to grow new branches, while only 3 (13.04%) of the seedlings in the *DcERF109* silenced group had grown a second shoot branch (Figure 6A,B). Two representative seedlings from each group were selected to test their gene expression levels. Compared with the control group, the expression of *DcERF109* was decreased, and *DcDAD2.2* was increased in the silenced seedlings (Figure 6C and 6D). These analyses showed that the reduced expression of *DcERF109* was caused by TRV carrying the *DcERF109* fragment, and in silenced seedlings, *DcERF109* reduced the inhibition of *DcDAD2.2*, resulting in the retarded growth of new shoot branches.

3.7 | *DpERF109* has a similar function in shoot branching and dwarfing

ERF109 has homologous genes in many species, including Orchids, Gramineae, Leguminosae, and others (Table S2). To investigate the evolutionary relationship between the *DcERF109* protein and other *ERF109* proteins, a phylogenetic tree that contains 33 species was constructed by MEGA X, revealing that the phylogeny of these

species is closely related to their speciation (Table S2). In the phylogenetic tree, 9 monocot plants are grouped into the same cluster. Three of the monocots (*D. catenatum*, *Dendrobium primulinum*, and *Phalaenopsis equestris*) that belong to Orchid plants are classified into the same sub-branch (Figure S6A). Through further sequence analysis, we found that they all have an AP2 domain near the C terminal, and the gene structure of *DpERF109* is most similar to that of *DcERF109*. The amino acid sequence alignment indicates that the homologous genes of *ERF109* in the three Orchid plants have high similarity in the AP2 domain, especially *DpERF109* (Figure S6B). Therefore, we suspected that *DpERF109* also has a similar function in plants. To verify this hypothesis, we cloned *DpERF109* from *D. primordium* and overexpressed it in *A. thaliana*. As shown in Figure S6C, we observed significant dwarfing and excessive shoot branching in *DpERF109*-OE plants. These results suggest that the *ERF109* homologous genes were highly conserved in Orchids and may have similar functions in orchids.

4 | DISCUSSION

Strigolactones (SLs), a class of plant hormones identified in recent years (Zwanenburg et al., 2016), play important roles in plant rhizosphere signal transduction (Tsuchiya and McCourt, 2012), host-

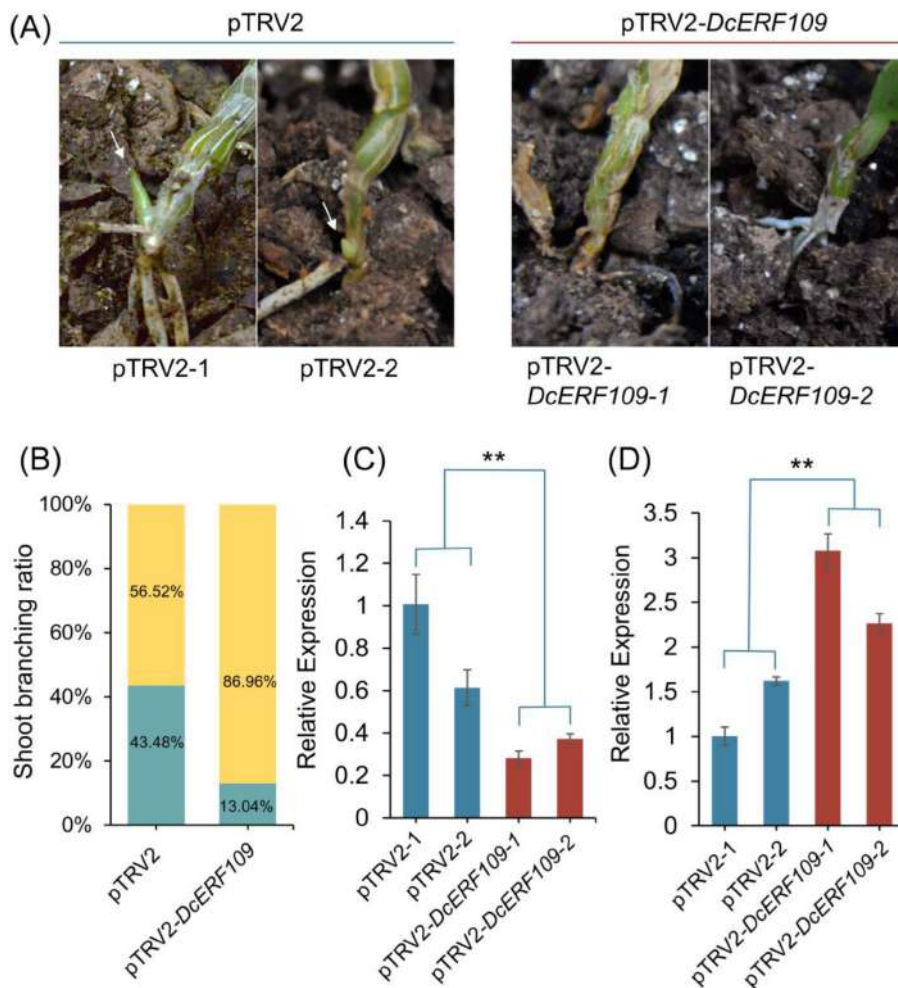


FIGURE 6 Silencing of *DcERF109* resulted in decreased shoot branching. **A**, Shoot branching phenotypes of pTRV2 and pTRV2-*DcERF109* silencing seedlings. White arrows indicate new branches. These photographs were taken 15 days after infiltration. **B**, Statistic analysis on the new shoot branching seedlings in pTRV2 and pTRV2-*DcERF109* groups. Yellow and blue represent the seedlings without new shoot branches and seedlings with new shoot branches, respectively. **C**, Expression of *DcERF109* in seedlings of pTRV2 and pTRV2-*DcERF109* groups. **D**, Expression of *DcDAD2.2* in seedlings of pTRV2 and pTRV2-*DcERF109* groups. Values are presented as means \pm SD (** $p < 0.01$, Student's *t*-test).

parasite interactions (Yoneyama et al., 2010), as well as plant dwarfing and shoot branching regulation (Chesterfield et al., 2020; Liang et al., 2010). However, few studies have shown the regulatory effect of SL in Orchid, particularly in the genus *Dendrobium*. The stem of *D. catenatum* bears significant economic and medicinal value. In this study, we have demonstrated evidence that the AP2/ERF family gene *DcERF109* affects the number of shoot branches by regulating the SL signal pathway. Firstly, we administered GR24^{rac} and TIS108 as substitutes and inhibitors of SL, respectively, to *D. catenatum* seedlings. The results substantiated that SL signals have a vital impact on shoot branching in *D. catenatum*. Secondly, we have demonstrated that there is a significant expression difference of the *DcDAD2.2*, a receptor of SL, in the stem base of multi-shoot branched and single-shoot branched *D. catenatum* seedlings and the expression level of *DcERF109* has almost the same times of reverse foldchange. Moreover, the ectopic overexpression of *DcERF109* in *A. thaliana* and knocked down expression of *DcERF109* in *D. catenatum* further elucidated its functional relevance. Conversely, VIGS-induced silencing of *DcERF109* in *D. catenatum* produced an antithetical branching phenotype. By Y1H and Luciferase reporter assays, we demonstrated that *DcERF109* directly binds and negatively regulates the expression of *AtD14* and *DcDAD2.2*. Moreover, we found the specificity of the Orchid *ERF109* gene and demonstrated that *DpERF109* can also cause an increase in shoot branches. These results deepen our understanding of SL signal and AP2/ERF family functions.

4.1 | The function of *ERF109* demonstrates interspecific variability

The *ERF109* transcription factor is represented by orthologous genes across a myriad of species, manifesting a spectrum of biological roles within plant defence and stress responses. In *A. thaliana*, *AtERF109* can respond to JA-mediated wound signals and prevent plant hypersensitivity by elevating *ASA1* expression and directly inhibiting JAZ proteins (Zhang and Zhao, 2019). Additionally, there is substantial evidence that *AtERF109/AtRRTF1* plays an important role in ROS production and auxin-mediated tissue repair within *A. thaliana* (Kong et al., 2018; J. Wang et al., 2020; Ye et al., 2020). The multifunctionality of *ERF109* extends to the regulation of secondary metabolite accumulation. As demonstrated in *Malus domestica* (apple), *MdERF109* modulates anthocyanin biosynthesis by interacting with *MdLNC499* and *MdWRKY1* (Ma et al., 2021). In *Poncirus trifoliata* (trifoliolate orange), *PtERF109* contributes to cold tolerance by directly regulating the expression of *Prx1* involved in the antioxidative process (Wang et al., 2019). Additional evidence indicates that *ERF109* also has implications for salt tolerance and SA signal response in plants (Bahieldin et al., 2018, 2016; Redwan et al., 2016). These clues suggest that *ERF109* has shaped distinct functional roles imperative for plant adaptation and survival. Therefore, understanding the conserved and unique aspects of *ERF109* function within each biological context holds substantial value for advancing agricultural biotechnology.

4.2 | *DcERF109* may have the ability to regulate other signal pathways

Among the characterization of transgenic *Arabidopsis* lines, we found that the expression level of *DcERF109* was positively correlated with the proliferation of shoot branches and negatively correlated with plant height. Notably, the plant architecture of *A. thaliana* has been completely changed among the highest expression levels of several lines (Figure S3 and Figure S4). Such marked phenotypic alterations are seemingly beyond the scope of SL regulation. Moreover, the phenotypes except shoot branching and dwarfing (Figure S3) prompt the conjecture that *DcERF109* may extend its regulatory influence to additional signalling cascades. In corroboration, previous investigations have illustrated that the loss-of-function mutant *mur3-3* in *A. thaliana* displays curled rosette leaves, abbreviated petioles, and stunted inflorescence stems due to a significant reduction in galactosylated xylose. Its phenotype is similar to those observed in the *DcERF109* overexpression lines (Kong et al., 2015). Conversely, the accumulation of ROS can cause oxidative stress, leading to severe damage to biological macromolecules such as proteins, lipids, and nucleic acids, ultimately leading to cell death (Gaber et al., 2012; Mittler, 2002). Compared to wild-type Col-0, the *DcERF109* overexpression lines displayed an elevated predisposition to wilting and oxidative damage (Figure 2A). The results contradict prior studies showing that SL promotes leaf ageing (Guo et al., 2021). Therefore, it is hypothesized that *DcERF109* may promote the accumulation of ROS within plant tissues through mechanisms distinct from SL-mediated pathways.

4.3 | Orchid *ERF109* proteins may bind TTG motif to regulate the expression of *AtD14* and *DcDAD2.2*

Many studies have pointed out that the AP2/ERF family has a strong binding ability to the GCC box, DRE box, and CRT box (Feng et al., 2020; Nakano et al., 2006; Riechmann and Meyerowitz, 1998). However, in our investigation, none of the aforementioned motifs were found in the promoter regions of *AtD14* and *DcDAD2.2*. Additionally, recent research has uncovered that ERF proteins can bind an alternate cis-acting element, the TTG motif (Qin et al., 2017). Comprehensive analysis of the cis-acting element displays a complete TTG2 (TTTTTTTGT) motif in the P4 fragment of the *AtD14* promoter and a truncated TTG1 (AACAAACA) motif in the P4 part of the *DcDAD2.2* promoter. These findings suggested that *DcERF109* may attenuate the expression of downstream target genes by binding to TTG motifs, which needed more experimental evidence to validate the binding ability of *DcERF109* to TTG motifs.

5 | CONCLUSION

In summary, our investigation has demonstrated that *DcERF109* modulates shoot branching by regulating the expression of *D14/DAD2.2*.

These insights advance the potential for genetic improvement of *Dendrobium* germplasm resources and serve to augment the economic value of this genus.

AUTHOR CONTRIBUTIONS

Tao Chen and Maohong Cai designed the experiments; Yuliang Han, Siqi Zhang, Lijun Xiang, Zhonghua Lei, Qixiu Huang performed the experiments; Juncheng Zhang analyzed the data; Yuliang Han and Huizhong Wang wrote and revised this article; all authors read and approved the final manuscript.

ACKNOWLEDGEMENTS

This work was supported by the Scientific Research Foundation for Scholars of HZNU (2019QDL015) and the Zhejiang Provincial Natural Science Foundation of China (Grant NO. LQ22C130001).

FUNDING INFORMATION

Scientific Research Foundation for Scholars of HZNU (2019QDL015). Zhejiang Provincial Natural Science Foundation of China (Grant NO. LQ22C130001).

DATA AVAILABILITY STATEMENT

The data supporting the findings of this study are available within the article and its supplementary materials.

ORCID

Maohong Cai  <https://orcid.org/0000-0002-7180-7659>

REFERENCES

- Bahieldin, A., Atef, A., Edris, S., Gadalla, N.O., Ali, H.M., Hassan, S.M., Al-Kordy, M.A., Ramadan, A.M., Makki, R.M., Al-Hajar, A.S.M., El-Domyati, F.M., 2016. Ethylene responsive transcription factor ERF109 retards PCD and improves salt tolerance in plant. *BMC Plant Biol.* 16, 216. <https://doi.org/10.1186/s12870-016-0908-z>
- Bahieldin, A., Atef, A., Edris, S., Gadalla, N.O., Ramadan, A.M., Hassan, S.M., Al Attas, S.G., Al-Kordy, M.A., Al-Hajar, A.S.M., Sabir, J.S.M., Nasr, M.E., Osman, G.H., El-Domyati, F.M., 2018. Multi-functional activities of ERF109 as affected by salt stress in *Arabidopsis*. *Sci. Rep.* 8, 6403. <https://doi.org/10.1038/s41598-018-24452-6>
- Bechtold, N., Pelletier, G., 1998. In planta *Agrobacterium*-mediated transformation of adult *Arabidopsis thaliana* plants by vacuum infiltration. *Methods Mol. Biol. Clifton NJ* 82, 259–266. <https://doi.org/10.1385/0-89603-391-0:259>
- Chai, D., Lee, S.M., Ng, J.H., Yu, H., 2007. L-methionine sulfoximine as a novel selection agent for genetic transformation of orchids. *J. Biotechnol.* 131, 466–472. <https://doi.org/10.1016/j.jbiotec.2007.07.951>
- Chandler, J.W., Werr, W., 2020. A phylogenetically conserved APETA-LA2/ETHYLENE RESPONSE FACTOR, ERF12, regulates *Arabidopsis* floral development. *Plant Mol. Biol.* 102, 39–54. <https://doi.org/10.1007/s11103-019-00936-5>
- Chen, C., Chen, H., Zhang, Y., Thomas, H.R., Frank, M.H., He, Y., Xia, R., 2020. TBtools: An Integrative Toolkit Developed for Interactive Analyses of Big Biological Data. *Mol. Plant* 13, 1194–1202. <https://doi.org/10.1016/j.molp.2020.06.009>
- Cheng, X., Floková, K., Bouwmeester, H., Ruyter-Spira, C., 2017. The Role of Endogenous Strigolactones and Their Interaction with ABA during the Infection Process of the Parasitic Weed *Phelipanche ramosa* in Tomato Plants. *Front. Plant Sci.* 8, 392. <https://doi.org/10.3389/fpls.2017.00392>
- Chesterfield, R.J., Vickers, C.E., Beveridge, C.A., 2020. Translation of Strigolactones from Plant Hormone to Agriculture: Achievements, Future Perspectives, and Challenges. *Trends Plant Sci.* 25, 1087–1106. <https://doi.org/10.1016/j.tplants.2020.06.005>
- de Jong, M., George, G., Ongaro, V., Williamson, L., Willetts, B., Ljung, K., McCulloch, H., Leyser, O., 2014. Auxin and strigolactone signaling are required for modulation of *Arabidopsis* shoot branching by nitrogen supply. *Plant Physiol.* 166, 384–395. <https://doi.org/10.1104/pp.114.242388>
- Feng, K., Hou, X.-L., Xing, G.-M., Liu, J.-X., Duan, A.-Q., Xu, Z.-S., Li, M.-Y., Zhuang, J., Xiong, A.-S., 2020. Advances in AP2/ERF super-family transcription factors in plant. *Crit. Rev. Biotechnol.* 40, 750–776. <https://doi.org/10.1080/07388551.2020.1768509>
- Gaber, A., Ogata, T., Maruta, T., Yoshimura, K., Tamoi, M., Shigeoka, S., 2012. The Involvement of *Arabidopsis* Glutathione Peroxidase 8 in the Suppression of Oxidative Damage in the Nucleus and Cytosol. *Plant Cell Physiol.* 53, 1596–1606. <https://doi.org/10.1093/pcp/pcs100>
- Guo, Y., Ren, G., Zhang, K., Li, Z., Miao, Y., Guo, H., 2021. Leaf senescence: progression, regulation, and application. *Mol. Hortic.* 1, 5. <https://doi.org/10.1186/s43897-021-00006-9>
- Hamiaux, C., Drummond, R.S.M., Janssen, B.J., Ledger, S.E., Cooney, J.M., Newcomb, R.D., Snowden, K.C., 2012. DAD2 Is an α/β Hydrolase Likely to Be Involved in the Perception of the Plant Branching Hormone, Strigolactone. *Curr. Biol.* 22, 2032–2036. <https://doi.org/10.1016/j.cub.2012.08.007>
- Han, Y., Cai, M., Zhang, S., Chai, J., Sun, M., Wang, Y., Xie, Q., Chen, Y., Wang, H., Chen, T., 2022. Genome-Wide Identification of AP2/ERF Transcription Factor Family and Functional Analysis of DcAP2/ERF#96 Associated with Abiotic Stress in *Dendrobium catenatum*. *Int. J. Mol. Sci.* 23, 13603. <https://doi.org/10.3390/ijms232113603>
- Harrop, T.W.R., Mantegazza, O., Luong, A.M., Béthune, K., Lorieux, M., Jouannic, S., Adam, H., 2019. A set of AP2-like genes is associated with inflorescence branching and architecture in domesticated rice. *J. Exp. Bot.* 70, 5617–5629. <https://doi.org/10.1093/jxb/erz340>
- Jiang, L., Liu, X., Xiong, G., Liu, H., Chen, F., Wang, L., Meng, X., Liu, G., Yu, H., Yuan, Y., Yi, W., Zhao, L., Ma, H., He, Y., Wu, Z., Melcher, K., Qian, Q., Xu, H.E., Wang, Y., Li, J., 2013. DWARF 53 acts as a repressor of strigolactone signalling in rice. *Nature* 504, 401–405. <https://doi.org/10.1038/nature12870>
- Kameoka, H., Dun, E.A., Lopez-Obando, M., Brewer, P.B., De Saint Germain, A., Rameau, C., Beveridge, C.A., Kozuka, J., 2016. Phloem Transport of the Receptor DWARF14 Protein Is Required for Full Function of Strigolactones. *Plant Physiol.* 172, 1844–1852. <https://doi.org/10.1104/pp.16.01212>
- Kerr, S.C., Patil, S.B., de Saint Germain, A., Pillot, J.-P., Saffar, J., Ligerot, Y., Aubert, G., Citerne, S., Bellec, Y., Dun, E.A., Beveridge, C.A., Rameau, C., 2021. Integration of the SMXL/D53 strigolactone signaling repressors in the model of shoot branching regulation in *Pisum sativum*. *Plant J. Cell Mol. Biol.* 107, 1756–1770. <https://doi.org/10.1111/tpj.15415>
- Kong, X., Tian, H., Yu, Q., Zhang, F., Wang, R., Gao, S., Xu, W., Liu, J., Shani, E., Fu, C., Zhou, G., Zhang, L., Zhang, X., Ding, Z., 2018. PHB3 Maintains Root Stem Cell Niche Identity through ROS-Responsive AP2/ERF Transcription Factors in *Arabidopsis*. *Cell Rep.* 22, 1350–1363. <https://doi.org/10.1016/j.celrep.2017.12.105>
- Kong, Y., Peña, M.J., Renna, L., Avci, U., Pattathil, S., Tuomivaara, S.T., Li, X., Reiter, W.-D., Brandizzi, F., Hahn, M.G., Darvill, A.G., York, W.S., O'Neill, M.A., 2015. Galactose-depleted xyloglucan is dysfunctional and leads to dwarfism in *Arabidopsis*. *Plant Physiol.* 167, 1296–1306. <https://doi.org/10.1104/pp.114.255943>
- Kumar, S., Stecher, G., Li, M., Knyaz, C., Tamura, K., 2018. MEGA X: Molecular Evolutionary Genetics Analysis across Computing Platforms.

- Mol. Biol. Evol.* 35, 1547–1549. <https://doi.org/10.1093/molbev/msy096>
- Liang, J., Zhao, L., Challis, R., Leyser, O., 2010. Strigolactone regulation of shoot branching in chrysanthemum (*Dendranthema grandiflorum*). *J. Exp. Bot.* 61, 3069–3078. <https://doi.org/10.1093/jxb/erq133>
- Licausi, F., Ohme-Takagi, M., Perata, P., 2013. APETALA2/Ethylene Responsive Factor (AP2/ERF) transcription factors: mediators of stress responses and developmental programs. *New Phytol.* 199, 639–649. <https://doi.org/10.1111/nph.12291>
- Lin, R., Ding, L., Casola, C., Ripoll, D.R., Feschotte, C., Wang, H., 2007. Transposase-derived transcription factors regulate light signaling in Arabidopsis. *Science* 318, 1302–1305. <https://doi.org/10.1126/science.1146281>
- Lu, S., Wang, J., Chitsaz, F., Derbyshire, M.K., Geer, R.C., Gonzales, N.R., Gwadz, M., Hurwitz, D.I., Marchler, G.H., Song, J.S., Thanki, N., Yamashita, R.A., Yang, M., Zhang, D., Zheng, C., Lanczycki, C.J., Marchler-Bauer, A., 2020. CDD/SPARCLE: the conserved domain database in 2020. *Nucleic Acids Res.* 48, D265–D268. <https://doi.org/10.1093/nar/gkz991>
- Ma, H., Yang, T., Li, Y., Zhang, J., Wu, T., Song, T., Yao, Y., Tian, J., 2021. The long noncoding RNA MdLNC499 bridges MdWRKY1 and MdERF109 function to regulate early-stage light-induced anthocyanin accumulation in apple fruit. *Plant Cell* 33, 3309–3330. <https://doi.org/10.1093/plcell/koab188>
- Mashiguchi, K., Seto, Y., Yamaguchi, S., 2021. Strigolactone biosynthesis, transport and perception. *Plant J. Cell Mol. Biol.* 105, 335–350. <https://doi.org/10.1111/tpj.15059>
- Mittler, R., 2002. Oxidative stress, antioxidants and stress tolerance. *Trends Plant Sci.* 7, 405–410. [https://doi.org/10.1016/S1360-1385\(02\)02312-9](https://doi.org/10.1016/S1360-1385(02)02312-9)
- Nakano, T., Suzuki, K., Fujimura, T., Shinshi, H., 2006. Genome-wide analysis of the ERF gene family in Arabidopsis and rice. *Plant Physiol.* 140, 411–432. <https://doi.org/10.1104/pp.105.073783>
- Qin, L., Wang, L., Guo, Y., Li, Y., Ümüt, H., Wang, Y., 2017. An ERF transcription factor from *Tamarix hispida*, ThCRF1, can adjust osmotic potential and reactive oxygen species scavenging capability to improve salt tolerance. *Plant Sci.* 265, 154–166. <https://doi.org/10.1016/j.plantsci.2017.10.006>
- Redwan, M., Spinelli, F., Marti, L., Weiland, M., Palm, E., Azzarello, E., Mancuso, S., 2016. Potassium fluxes and reactive oxygen species production as potential indicators of salt tolerance in *Cucumis sativus*. *Funct. Plant Biol. FPB* 43, 1016–1027. <https://doi.org/10.1071/FP16120>
- Riechmann, J.L., Meyerowitz, E.M., 1998. The AP2/EREBP family of plant transcription factors. *Biol. Chem.* 379, 633–646. <https://doi.org/10.1515/bchm.1998.379.6.633>
- Simons, J.L., Napoli, C.A., Janssen, B.J., Plummer, K.M., Snowden, K.C., 2007. Analysis of the DECREASED APICAL DOMINANCE genes of petunia in the control of axillary branching. *Plant Physiol.* 143, 697–706. <https://doi.org/10.1104/pp.106.087957>
- Tsuchiya, Y., McCourt, P., 2012. Strigolactones as small molecule communicators. *Mol. Biosyst.* 8, 464–469. <https://doi.org/10.1039/c1mb05195d>
- Wang, J., Nan, N., Shi, L., Li, N., Huang, S., Zhang, A., Liu, Y., Guo, P., Liu, B., Xu, Z.-Y., 2020. Arabidopsis BRCA1 represses RRTF1-mediated ROS production and ROS-responsive gene expression under dehydration stress. *New Phytol.* 228, 1591–1610. <https://doi.org/10.1111/nph.16786>
- Wang, L., Wang, B., Jiang, L., Liu, X., Li, X., Lu, Z., Meng, X., Wang, Y., Smith, S.M., Li, J., 2015. Strigolactone Signaling in Arabidopsis Regulates Shoot Development by Targeting D53-Like SMXL Repressor Proteins for Ubiquitination and Degradation. *Plant Cell* 27, 3128–3142. <https://doi.org/10.1105/tpc.15.00605>
- Wang, L., Wang, B., Yu, H., Guo, H., Lin, T., Kou, L., Wang, A., Shao, N., Ma, H., Xiong, G., Li, X., Yang, J., Chu, J., Li, J., 2020. Transcriptional regulation of strigolactone signalling in Arabidopsis. *Nature* 583, 277–281. <https://doi.org/10.1038/s41586-020-2382-x>
- Wang, M., Dai, W., Du, J., Ming, R., Dahro, B., Liu, J.-H., 2019. ERF109 of trifoliate orange (*Poncirus trifoliata* (L.) Raf.) contributes to cold tolerance by directly regulating expression of Prx1 involved in antioxidative process. *Plant Biotechnol. J.* 17, 1316–1332. <https://doi.org/10.1111/pbi.13056>
- Wang, Q., Smith, S.M., Huang, J., 2022. Origins of strigolactone and karrikin signaling in plants. *Trends Plant Sci.* 27, 450–459. <https://doi.org/10.1016/j.tplants.2021.11.009>
- Wang, S., Guo, T., Wang, Z., Kang, J., Yang, Q., Shen, Y., Long, R., 2020. Expression of Three Related to ABI3/VP1 Genes in *Medicago truncatula* Caused Increased Stress Resistance and Branch Increase in Arabidopsis thaliana. *Front. Plant Sci.* 11, 611. <https://doi.org/10.3389/fpls.2020.00611>
- Wang, Y., Du, F., Wang, J., Wang, K., Tian, C., Qi, X., Lu, F., Liu, X., Ye, X., Jiao, Y., 2022. Improving bread wheat yield through modulating an unselected AP2/ERF gene. *Nat. Plants* 8, 930–939. <https://doi.org/10.1038/s41477-022-01197-9>
- Wang, Yue, Tong, Y., Adejobi, O.I., Wang, Yuhua, Liu, A., 2021. Research Advances in Multi-Omics on the Traditional Chinese Herb *Dendrobium officinale*. *Front. Plant Sci.* 12, 808228. <https://doi.org/10.3389/fpls.2021.808228>
- Xie, Y., Liu, Y., Wang, Hai, Ma, X., Wang, B., Wu, G., Wang, Haiyang, 2017. Phytochrome-interacting factors directly suppress MIR156 expression to enhance shade-avoidance syndrome in Arabidopsis. *Nat. Commun.* 8, 348. <https://doi.org/10.1038/s41467-017-00404-y>
- Xu, Y., Wang, J., Wang, R., Wang, L., Zhang, C., Xu, W., Wang, S., Jiu, S., 2021. The Role of Strigolactones in the Regulation of Root System Architecture in Grapevine (*Vitis vinifera* L.) in Response to Root-Restriction Cultivation. *Int. J. Mol. Sci.* 22, 8799. <https://doi.org/10.3390/ijms22168799>
- Yan, L., Wang, Xiao, Liu, H., Tian, Y., Lian, J., Yang, R., Hao, S., Wang, Xuanjun, Yang, S., Li, Q., Qi, S., Kui, L., Okpekum, M., Ma, X., Zhang, J., Ding, Z., Zhang, G., Wang, W., Dong, Y., Sheng, J., 2015. The Genome of *Dendrobium officinale* Illuminates the Biology of the Important Traditional Chinese Orchid Herb. *Mol. Plant* 8, 922–934. <https://doi.org/10.1016/j.molp.2014.12.011>
- Yao, R., Ming, Z., Yan, L., Li, S., Wang, F., Ma, S., Yu, C., Yang, M., Chen, Li, Chen, Linhai, Li, Y., Yan, C., Miao, D., Sun, Z., Yan, J., Sun, Y., Wang, L., Chu, J., Fan, S., He, W., Deng, H., Nan, F., Li, J., Rao, Z., Lou, Z., Xie, D., 2016. DWARF14 is a non-canonical hormone receptor for strigolactone. *Nature* 536, 469–473. <https://doi.org/10.1038/nature19073>
- Ye, B.-B., Shang, G.-D., Pan, Y., Xu, Z.-G., Zhou, C.-M., Mao, Y.-B., Bao, N., Sun, L., Xu, T., Wang, J.-W., 2020. AP2/ERF Transcription Factors Integrate Age and Wound Signals for Root Regeneration. *Plant Cell* 32, 226–241. <https://doi.org/10.1105/tpc.19.00378>
- Yoneyama, Koichi, Awad, A.A., Xie, X., Yoneyama, Kaori, Takeuchi, Y., 2010. Strigolactones as germination stimulants for root parasitic plants. *Plant Cell Physiol.* 51, 1095–1103. <https://doi.org/10.1093/pcp/pcq055>
- Yu, B., Gruber, M.Y., Khachatourians, G.G., Zhou, R., Epp, D.J., Hegedus, D.D., Parkin, I.A.P., Welsch, R., Hannoufa, A., 2012. Arabidopsis cpSRP54 regulates carotenoid accumulation in Arabidopsis and Brassica napus. *J. Exp. Bot.* 63, 5189–5202. <https://doi.org/10.1093/jxb/ers179>
- zhang, G., Zhao, F., 2019. Jasmonate-mediated wound signalling promotes plant regeneration. *Nat. Plants.* <https://doi.org/10.1038/s41477-019-0408-x>
- Zhang, X., Henriques, R., Lin, S.-S., Niu, Q.-W., Chua, N.-H., 2006. Agrobacterium-mediated transformation of Arabidopsis thaliana using the floral dip method. *Nat. Protoc.* 1, 641–646. <https://doi.org/10.1038/nprot.2006.97>

Zwanenburg, B., Pospíšil, T., Čavar Zeljković, S., 2016. Strigolactones: new plant hormones in action. *Planta* 243, 1311–1326. <https://doi.org/10.1007/s00425-015-2455-5>

SUPPORTING INFORMATION

Additional supporting information can be found online in the Supporting Information section at the end of this article.

How to cite this article: Han, Y., Zhang, J., Zhang, S., Xiang, L., Lei, Z., Huang, Q. et al. (2024) *DcERF109* regulates shoot branching by participating in strigolactone signal transduction in *Dendrobium catenatum*. *Physiologia Plantarum*, 176(2), e14286. Available from: <https://doi.org/10.1111/ppl.14286>